

# Water Diffusion Changes in Wallerian Degeneration and Their Dependence on White Matter Architecture

Carlo Pierpaoli,\* Alan Barnett,† Sinisa Pajevic,‡ Robert Chen,§ LaRoy Penix,§  
Anette Virta,§ and Peter Basser\*

\*National Institute of Child Health and Human Development, †National Institute of Mental Health, ‡Center for Information Technology, and §National Institute of Neurological Disorders and Stroke, National Institutes of Health, Bethesda, Maryland 20892-5772

Received September 27, 2000

**This study investigates water diffusion changes in Wallerian degeneration. We measured indices derived from the diffusion tensor (DT) and T2-weighted signal intensities in the descending motor pathways of patients with small chronic lacunar infarcts of the posterior limb of the internal capsule on one side. We compared these measurements in the healthy and lesioned sides at different levels in the brainstem caudal to the primary lesion. We found that secondary white matter degeneration is revealed by a large reduction in diffusion anisotropy only in regions where fibers are arranged in isolated bundles of parallel fibers, such as in the cerebral peduncle. In regions where the degenerated pathway crosses other tracts, such as in the rostral pons, paradoxically there is almost no change in diffusion anisotropy, but a significant change in the measured orientation of fibers. The trace of the diffusion tensor is moderately increased in all affected regions. This allows one to differentiate secondary and primary fiber loss where the increase in trace is considerably higher. We show that DT-MRI is more sensitive than T2-weighted MRI in detecting Wallerian degeneration. Significant diffusion abnormalities are observed over the entire trajectory of the affected pathway in each patient. This finding suggests that mapping degenerated pathways noninvasively with DT-MRI is feasible. However, the interpretation of water diffusion data is complex and requires *a priori* information about anatomy and architecture of the pathway under investigation. In particular, our study shows that in regions where fibers cross, existing DT-MRI-based fiber tractography algorithms may lead to erroneous conclusion about brain connectivity.**

**Key Words:** diffusion; tensor; MRI; anisotropy; white matter; Wallerian; degeneration; brain; human.

## INTRODUCTION

Degeneration of white matter fibers at a distance from a primary lesion is a common finding in many

diseases of the Central Nervous System (CNS). Moreover, the study of degeneration of specific pathways, both in animal models and postmortem in human subjects with focal brain lesions has contributed greatly to our knowledge of neural connections between different regions in the CNS (See Jones, 1999) for a review).

Secondary white matter degeneration is classically divided into retrograde and anterograde (or Wallerian) degeneration. From the primary lesion, retrograde degeneration proceeds proximally toward the cell body, while anterograde degeneration proceeds distally toward the axon's terminals.

The ability to investigate secondary white matter fiber degeneration noninvasively would be valuable not only to improve diagnosis of many neurological diseases, but also to facilitate the study of human functional neuroanatomy. Conventional imaging techniques such as computed tomography (CT) and magnetic resonance imaging (MRI) can sometimes reveal changes in brain regions where secondary fiber degeneration has occurred. CT reveals white matter degeneration when atrophy is severe enough to produce significant volumetric changes (Stovring and Fernando, 1983). MRI may show increased T2 weighted signal intensity of the affected tracts even if atrophy is not severe (Cobb and Mehringer, 1987; Kuhn *et al.*, 1988, 1989). Unfortunately MRI signal changes produced by Wallerian degeneration are often small and not consistently present in all subjects (Sawhani *et al.*, 1997).

MRI can also be used to investigate the diffusion properties of tissue water (See Le Bihan, 1991, for a review). Previous studies have shown that water diffusion may be altered in white matter tracts following Wallerian degeneration (Segawa *et al.*, 1993; Beaulieu *et al.*, 1996; Pierpaoli *et al.*, 1996a, 1998; Makris *et al.*, 1997; Tievsky *et al.*, 1998; Castillo and Mukherji, 1999; Wiesmann *et al.*, 1999a, b). Normal white matter tracts with coherently oriented fibers show high diffusion anisotropy, in particular a higher diffusivity in the direction parallel to the fibers than in the direction perpendicular to them. One common finding in Walle-

rian degeneration is that diffusion anisotropy is reduced. This change is thought to originate from structural changes in the tissue, such as loss of axons and gliosis. However, architectural features of the tissue, such as the degree of orientational coherence of fibers, are also known to affect diffusion anisotropy (Pierpaoli and Basser, 1996; Pierpaoli *et al.*, 1996b; Virta *et al.*, 1999). In normal white matter, for example, regions such as the corpus callosum and cerebral peduncle, where fibers are coherently oriented within the voxel, have higher diffusion anisotropy than regions such as the centrum semiovale and other subcortical areas, where the orientation of fibers within a voxel is less coherent. Recently, it was demonstrated that structural changes occurring in white matter with aging are reflected by changes in tissue diffusion properties that depend on the local architectural arrangement of white matter fibers (Virta *et al.*, 1999). We hypothesized that changes in diffusion properties produced by Wallerian degeneration may also have different manifestations depending upon white matter architecture in the affected region.

To investigate this hypothesis we studied the descending motor pathways of patients that had a small lacunar infarct in the posterior limb of either the left or right internal capsule using diffusion tensor MRI (see Basser, 1995, for a review). The normal structure and architecture of the descending motor pathways is well known, and previous DT-MRI studies have already characterized the diffusion properties of these pathways in normal subjects (Virta *et al.*, 1999). In particular it has been demonstrated that no differences in diffusion parameters can be found in normal subjects between tracts on the left and right sides. This allows one to use the contralateral unaffected tract as an internal control for the assessment of changes produced in Wallerian degeneration.

The diffusion parameters that we investigate include: the principal diffusivities (eigenvalues of  $\mathbf{D}$ ), the Trace of the diffusion tensor (Trace( $\mathbf{D}$ )), indices of diffusion anisotropy, and the principal directions of diffusion (eigenvectors of  $\mathbf{D}$ ). In addition to these diffusion parameters, we measured the T2-weighted signal intensity in all anatomical regions of interest to compare the sensitivity of DT-MRI- and T2-weighted imaging in detecting Wallerian degeneration.

## METHODS

### *Experimental Design*

In our experiment, we investigate a pathway that has a well-known structure and architecture. We include only subjects with focal infarcts in the posterior limb of the internal capsule to assure that the observed changes were caused by selective involvement of the descending motor pathways and not by more global

degenerative changes that are likely to occur in larger strokes. Finally, we include only subjects that had the stroke at least 1 year before the scan to assure that Wallerian degeneration was in its chronic stage. Seven subjects were included in the study (Six males, one female, age range 50–75, mean age  $\pm$  SD:  $64 \pm 9$  years). Inclusion criteria were: (a) History of capsular stroke occurring at least 1 year before the inclusion in the study, (b) Neurological evaluation indicating unilateral signs of motor impairment without cognitive impairment, (c) MRI evidence of one or more focal lesions in the posterior limb of either the left or right internal capsule, and (d) Absence of gross signal abnormalities in other regions of the brain, in particular in the contralateral internal capsule and in the brainstem. Small focal hyperintensities in regions distant from the descending motor pathways were accepted since this finding is very common in the T2-weighted images of healthy elderly subjects (Wahlund *et al.*, 1996; Salonen *et al.*, 1997).

### *MRI*

All imaging studies were performed with a 1.5 T GE Signa Horizon EchoSpeed spectrometer, equipped with a whole-body gradient coil able to produce gradient pulses up to 22 mT/m and a birdcage quadrature radiofrequency coil (GE Medical Systems, Milwaukee, WI). Head motion was reduced by placing pads on both sides of the subject's head. Diffusion images were acquired using an interleaved spin-echo echo-planar imaging sequence with a navigator echo to correct motion artifacts (Anderson and Gore, 1994; Ordidge *et al.*, 1994). A description of the algorithms used for image reconstruction is presented elsewhere (Barnett, 1997; Jezzard *et al.*, 1998). Typical acquisition parameters were: 30–33 contiguous axial slices; 3.5-mm slice thickness; 220-mm field of view;  $128 \times 128$  in-plane resolution (8 interleaves, 16 echoes per interleaf); echo-time of 78 ms; and repetition time of greater than 5 s with cardiac gating (3–4 acquisitions per heart beat starting with a 200 ms delay after the rise of the sphygmoc wave as measured with a peripheral pulse oxymeter). The signal to noise ratio achieved in normal brain parenchyma using these parameters ranged between 25 and 35 in the images with no diffusion weighting. Six logical gradient directions were sampled according to the scheme presented in (Pierpaoli *et al.*, 1996b), with four images acquired for each direction at maximum gradient strength (21 mT/m), yielding an effective “*b* value” (i.e., Trace of the *b* matrix (Mattiello *et al.*, 1997)) of  $1006 \text{ s/mm}^2$ . Four images with no diffusion weighting were also acquired for a total of 28 images per slice. The total imaging time was approximately 30–40 min, depending on the subject's heart rate. Following image reconstruction, the diffusion tensor ( $\mathbf{D}$ ) in each voxel was calculate according to Basser *et al.* (1994) using a

numerically computed  $b$  matrix for each image (Mattiello *et al.*, 1997). From  $\mathbf{D}$  we computed maps of the three principal diffusivities (eigenvalues of  $\mathbf{D}$ )  $\lambda_1$ ,  $\lambda_2$ , and  $\lambda_3$ ,  $\text{Trace}(\mathbf{D})$ , the principal directions of diffusion (eigenvectors of  $\mathbf{D}$ ), the “fractional” anisotropy index (Basser and Pierpaoli, 1996) and the “lattice” anisotropy index (Pierpaoli and Basser, 1996). The lattice anisotropy index is a rotationally invariant measure of diffusion anisotropy that is relatively immune to bias induced by noise in the diffusion-weighted images.<sup>1</sup> Color maps of fiber orientation were produced using the “absolute value” scheme described by Pajevic and Pierpaoli (1999). Fiber tract trajectories were calculated from the diffusion tensor data using a fiber tractography algorithm described in (Basser, 1998; Aldroubi and Basser, 1999; Basser *et al.*, 2000). These fiber tract trajectories are determined as follows. First, a continuous diffusion tensor field is constructed from the discrete, noisy, measured DT-MRI data. Then, a continuous representation of the fiber direction (vector) field is obtained from this continuous tensor field assuming that the local fiber tract directions coincide with the direction of largest diffusivity. Then a Frenet equation, describing the evolution of a 3-D fiber tract, is solved numerically within the imaging volume.

#### Data Analysis

Regions of interest (ROIs) were manually drawn on the T2-weighted images obtained by averaging the four replicate images acquired without diffusion weighting. The measurement of T2-weighted signal intensities was also performed on these images, rather than on high resolution fast spin echo images, because these images are perfectly coregistered with the maps of the quantities derived from the diffusion tensor allowing the use of the same ROIs for analysis of both T2-weighted and diffusion data. ROIs were drawn on the left and right descending motor pathways at the level of the primary lesion and on all slices in the brainstem caudal to the primary lesion to a level just above the pyramidal decussation. Data from contiguous slices were pooled to form five anatomical ROIs: primary lesion (1 or 2 slices), internal capsule caudal to the primary lesion (2 slices), cerebral peduncle (3 slices), rostral pons (2 slices), and caudal pons (2 slices). Given the close proximity of the left and right tracts in the medulla and the relatively low resolution of our images, the separation between ipsilateral and contralateral ROIs would be somewhat arbitrary at the level of the medulla. For this reason we did not perform a quantitative statistical analysis in the medulla. However, we present maps of diffusion quantities where

differences between the side ipsilateral to the lesion (affected side) and the contralateral side (healthy side) are apparent by visual inspection. Differences between the affected side and the healthy side in these five anatomical ROIs were assessed using the Mann–Whitney test with and without Bonferroni correction for multiple comparisons. Statistics were computed with a threshold for statistical significance set at  $P = 0.01$ . The Mann–Whitney test, which is the nonparametric analog of the Student’s  $t$  test, was chosen because the distribution of some diffusion parameters, such as diffusion anisotropy, is non-Gaussian (Pierpaoli and Basser, 1996; Pajevic and Basser, 1999). Moreover, tissue inhomogeneity within the ROI may also contribute to a non-Gaussian distribution of values.

## RESULTS

Table 1 shows values of the T2-weighted signal intensity, orientationally averaged diffusion coefficient ( $\text{Dav} = 1/3 \text{Trace}(\mathbf{D})$ ), diffusion anisotropy, and principal diffusivities for the healthy and affected sides. These values are obtained by averaging all voxels of all subjects within each ROI. ROIs were drawn in the internal capsule at the level of the stroke lesion (Primary lesion ROI) and in four other regions caudal to the primary lesion where Wallerian degeneration of the descending motor fibers had occurred. In the primary lesion, T2-weighted signal intensity (T2SI),  $\text{Trace}(\mathbf{D})$ , and principal diffusivities values are greatly increased with respect to the healthy side, while diffusion anisotropy is strongly reduced. In the ROIs caudal to the primary lesion where Wallerian degeneration has occurred (internal capsule, cerebral peduncle, rostral pons, caudal pons) T2SI and  $\text{Trace}(\mathbf{D})$  show much smaller differences between the affected and healthy sides with only a slight increase in the affected side that does not exceed 10% for T2SI and 18% for  $\text{Trace}(\mathbf{D})$ . Diffusion anisotropy, however, is sharply reduced with the lattice anisotropy index decreasing more than 40% in all ROIs except within the rostral pons where anisotropy is reduced by only 11%. In all ROIs with secondary white matter degeneration the reduction in diffusion anisotropy results from a decrease of the largest principal diffusivity,  $\lambda_1$ , and an increase of the intermediate and smallest principal diffusivities,  $\lambda_2$  and  $\lambda_3$ . This finding is in contrast with diffusion changes observed in the primary lesion where diffusion anisotropy is also reduced but all three principal diffusivities,  $\lambda_1$ ,  $\lambda_2$ , and  $\lambda_3$  increase.

When the entire data set except the primary lesion ROI was pooled, the Mann–Whitney test revealed significant differences in T2SI,  $\text{Trace}(\mathbf{D})$ , and diffusion anisotropy between the healthy and affected sides. This result indicates that T2SI,  $\text{Trace}(\mathbf{D})$ , and diffusion anisotropy were all sensitive enough to reveal overall differences produced by Wallerian degeneration be-

<sup>1</sup> The formula of the lattice index contained typographical errors in the original publication (Pierpaoli and Basser, 1996). The correct formula is reported in (Pajevic and Pierpaoli, 1999; Virta *et al.* 1999).

TABLE 1

Comparison between Healthy and Affected Side for T2-Weighted Signal Intensity (T2SI), Orientationally Averaged Diffusion Coefficient, Fractional and Lattice Anisotropy Indices, and the Three Principal Diffusivities of **D**

	Primary stroke lesion		Secondary white matter degeneration							
	Internal capsule		Internal capsule		Cerebral peduncle		Rostral pons		Caudal pons	
	Healthy side	Affected side	Healthy side	Affected side	Healthy side	Affected side	Healthy side	Affected side	Healthy side	Affected side
T2SI (Arbitrary units)	100 ± 5	220 ± 45	100 ± 10	109 ± 23	100 ± 9	100 ± 18	100 ± 7	103 ± 11	100 ± 6	107 ± 10
$D_{av} = \text{Trace}(\mathbf{D})/3$ ( $\times 10^{-9} \text{ m}^2/\text{s}$ )	0.75 ± 0.07	2.27 ± 0.63	0.72 ± 0.09	0.85 ± 0.16	0.76 ± 0.08	0.83 ± 0.14	0.72 ± 0.08	0.75 ± 0.11	0.76 ± 0.08	0.84 ± 0.11
Diffusion anisotropy (dimensionless)										
Lattice anisotropy index	0.51 ± 0.07	0.10 ± 0.11	0.59 ± 0.10	0.28 ± 0.12	0.61 ± 0.09	0.36 ± 0.13	0.35 ± 0.11	0.31 ± 0.10	0.31 ± 0.10	0.18 ± 0.08
Fractional anisotropy index	0.68 ± 0.07	0.20 ± 0.15	0.76 ± 0.09	0.46 ± 0.15	0.76 ± 0.09	0.52 ± 0.15	0.53 ± 0.13	0.49 ± 0.13	0.55 ± 0.13	0.39 ± 0.12
Principal diffusivities ( $\times 10^{-9} \text{ mm}^2/\text{s}$ )										
Largest ( $\lambda_1$ )	1.42 ± 0.16	2.66 ± 0.57	1.51 ± 0.20	1.30 ± 0.24	1.61 ± 0.18	1.37 ± 0.25	1.18 ± 0.20	1.17 ± 0.21	1.27 ± 0.24	1.18 ± 0.17
Intermediate ( $\lambda_2$ )	0.57 ± 0.12	2.22 ± 0.70	0.46 ± 0.15	0.75 ± 0.20	0.44 ± 0.12	0.68 ± 0.18	0.67 ± 0.14	0.71 ± 0.17	0.67 ± 0.14	0.81 ± 0.14
Lowest ( $\lambda_3$ )	0.25 ± 0.09	1.91 ± 0.66	0.20 ± 0.10	0.49 ± 0.20	0.23 ± 0.11	0.44 ± 0.17	0.33 ± 0.12	0.38 ± 0.13	0.35 ± 0.12	0.52 ± 0.14

*Note.* Results are reported for the stroke lesion (Primary lesion) and for four other anatomical regions caudal to the primary lesion where Wallerian degeneration of the descending motor fibers had occurred. Mean values ± standard deviations are obtained by pooling ROIs in corresponding anatomical regions in all subjects. In each ROI, T2SI is normalized with respect to the mean value of the healthy side that is set to 100.

tween the healthy and affected sides when the entire study population was considered. However, when the Mann–Whitney test was applied to each patient individually, only diffusion anisotropy revealed significant differences between the healthy and affected sides in all subjects. No significant differences were found in four subjects for T2SI and in one subject for Trace(**D**).

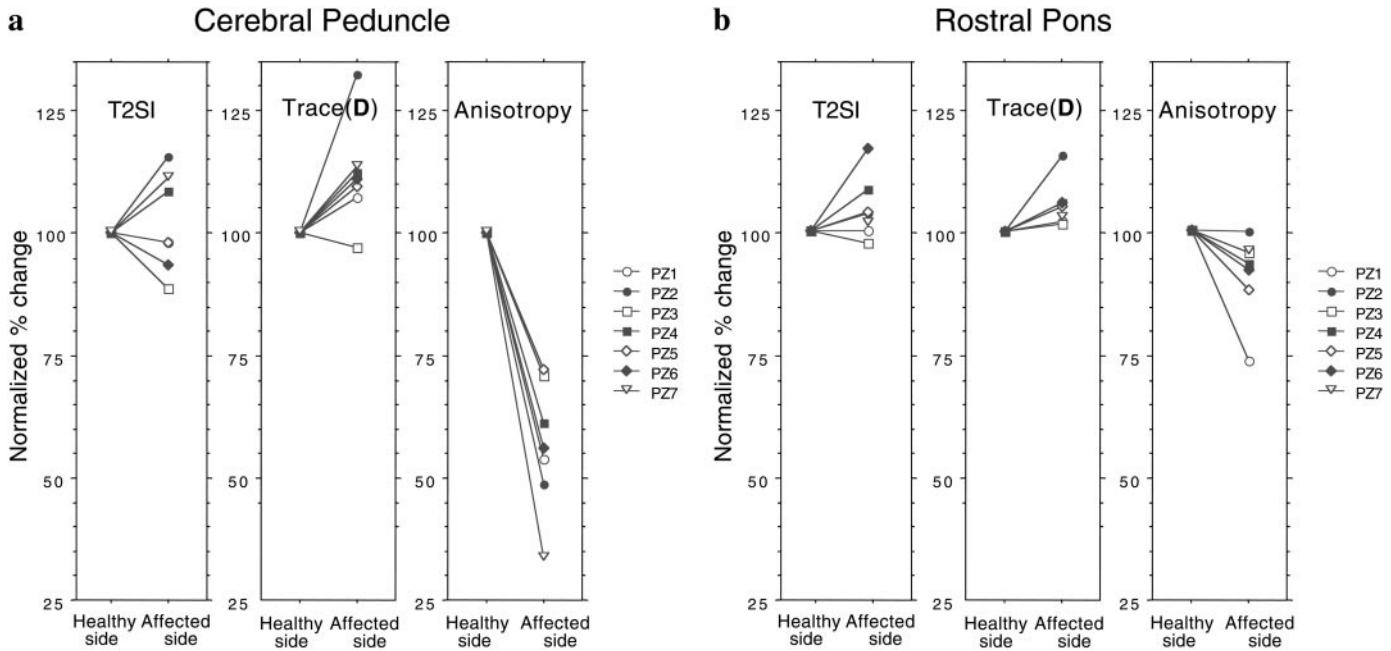
The analysis was extended to investigate differences between the healthy and affected sides within each ROI in each patient. We performed 28 comparisons, since we defined 4 ROIs at different levels of the cortico-spinal tract caudal to the primary lesion, and we studied 7 patients. Even without Bonferroni correction the sensitivity of the T2SI was very low with only 10 of 28 comparisons showing significant differences between the healthy and affected sides. Trace(**D**) showed 18 significant differences and the lattice anisotropy index showed 25 significant differences. All three comparisons in which the lattice anisotropy index in the affected side was not significantly reduced were in the rostral pons. When Bonferroni correction was applied, the number of significantly different comparisons dropped to 6, 11, and 22 for the T2SI, Trace(**D**), and the lattice anisotropy index, respectively. Again, all ROIs with no significant differences in diffusion anisotropy were in the pons.

Figure 1 shows the percentage changes of T2SI, Trace(**D**), and Lattice index in the affected side for each patient in two ROIs, the cerebral peduncle (Fig. 1a) and the rostral pons (Fig. 1b). T2SI and Trace(**D**) show only small differences between healthy and affected

sides in both ROIs. In the cerebral peduncle, Wallerian degeneration could not be reliably identified in the T2-weighted images given that changes in T2SI in the affected side are inconsistent, increasing in three subjects but decreasing in the other four. In contrast, diffusion anisotropy was consistently reduced in all seven subjects. These findings in the cerebral peduncle are representative of findings in the internal capsule and in the caudal pons. In the rostral pons, however, diffusion anisotropy was reduced by a lesser degree than in all other regions and even showed a slight increase in one subject.

Figures 2 and 3 show T2-weighted images, maps of Trace(**D**), and maps of the lattice anisotropy index of one representative subject at the level of the primary lesion and for different levels in the brainstem caudal to the primary lesion. The primary lesion is easily identified as an area of increased T2SI, increased Trace(**D**), and severely reduced diffusion anisotropy (arrows). Differences between healthy and affected sides are more difficult to detect in the brainstem caudal to the lesion in both T2SI and Trace(**D**) maps. Diffusion anisotropy is clearly reduced in the affected side at the level of the cerebral peduncle, caudal pons, and medulla. Interestingly, In the cerebral peduncle, the topographic localization of the degenerated fibers can be seen in the anisotropy map. Diffusion anisotropy does not appear clearly reduced in the rostral pons.

Figure 4 shows direction-encoded color (DEC) maps (Pierpaoli, 1997; Pajevic and Pierpaoli, 1999) obtained



**FIG. 1.** T2SI, Trace(D), and Lattice anisotropy index changes in the side ipsilateral to the lesion expressed as a percentage of the values measured in the side contralateral to the lesion in both the cerebral peduncle (a) and the rostral pons (b). While changes in T2SI and Trace(D) show similar trends in the cerebral peduncle and in the rostral pons, a large reduction in diffusion anisotropy is observed only in the cerebral peduncle but not in the rostral pons.

from of the same subjects shown in Figs. 2 and 3. In these maps bright voxels correspond to regions where water diffusion is anisotropic, while dark voxels indicate regions where water diffusion is isotropic. Different colors are associated with different fiber tract directions as indicated in the color circle shown in the top right of the figure. The left–right, anterior–posterior, and superior–inferior directions are, respectively, as-

sociated with pure red, green, and blue. Obliquely oriented fibers will be represented by colors resulting from a combination of red, green, and blue. The motor pathways generally have a magenta hue in the cerebral peduncle and a blue hue in the rest of the brainstem because of their predominantly rostral-caudal orientation. The red voxels in the rostral pons correspond to the transverse pontine fibers that have a predomi-

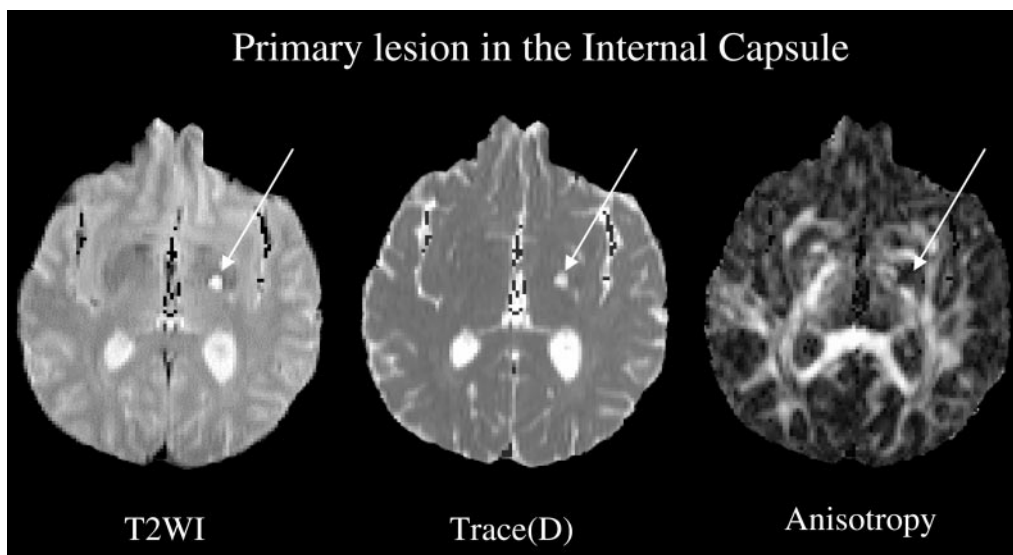
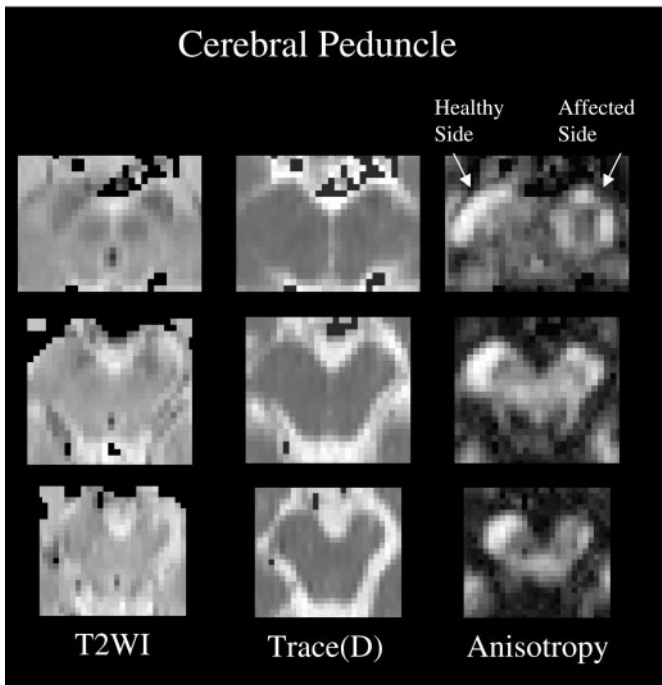
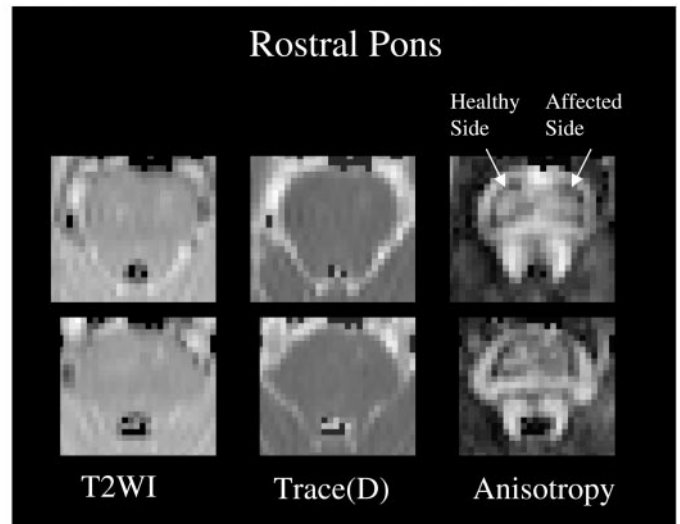


**FIG. 2.** T2-weighted image (T2WI), Trace(D) map, and lattice anisotropy index map of the brain of one representative subject at the level of the primary stroke lesion. The lesion is visible as an area of increased T2SI, increased Trace(D), and severely reduced anisotropy (arrows).

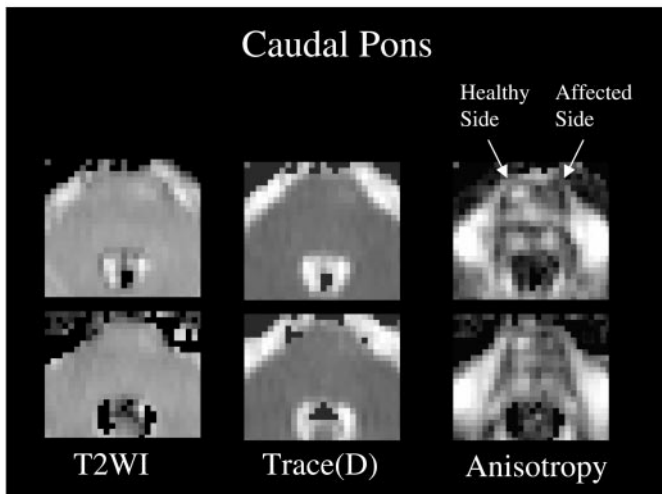
a



b



c



d

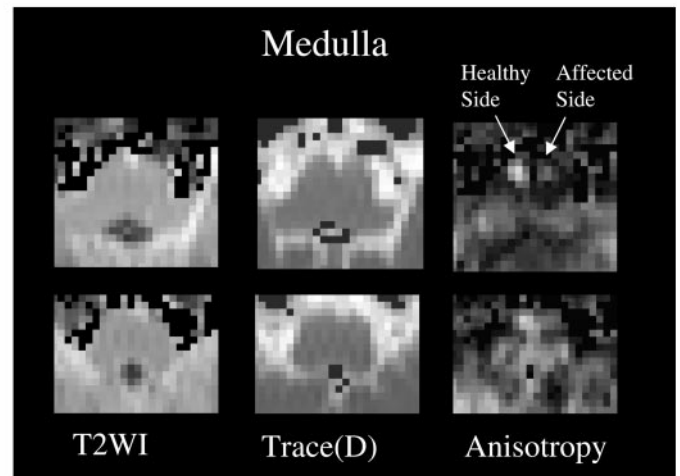


**FIG. 3.** T2-weighted images (T2WI), Trace(D) maps, and lattice anisotropy index maps of the brainstem caudal to the primary lesion in the same subject shown in Fig. 2. Three contiguous slices are shown in the cerebral peduncle (a), and two contiguous slices are shown in the rostral pons (b), caudal pons (c), and medulla (d). Arrows in the top anisotropy map of each figure indicate the location of the motor pathways.

nant left–right orientation. In the cerebral peduncle, caudal pons, and medulla, diffusion anisotropy of the motor pathways is lower in the affected side than in the healthy side (reduced brightness in the affected side). In contrast, in the rostral pons in the affected side diffusion anisotropy is not markedly reduced (healthy and affected side have similar brightness); however, fibers are more predominantly left–right oriented (the number of voxels with reddish hue (arrowhead) is

higher). This apparent change in direction of the motor pathways at the level of the rostral pons was found for all subjects studied by analyzing the components of the eigenvector,  $\epsilon_1$ , associated with the largest principal diffusivity. Overall the absolute value of the rostral-caudal component of  $\epsilon_1$ ,  $\epsilon_{1z}$ , decreased from  $0.71 \pm 0.24$  in the healthy side to  $0.53 \pm 0.30$  in the affected side and the absolute value of the left–right component of  $\epsilon_1$ ,  $\epsilon_{1x}$ , increased from  $0.46 \pm 0.28$  to  $0.60 \pm 0.31$ . In all

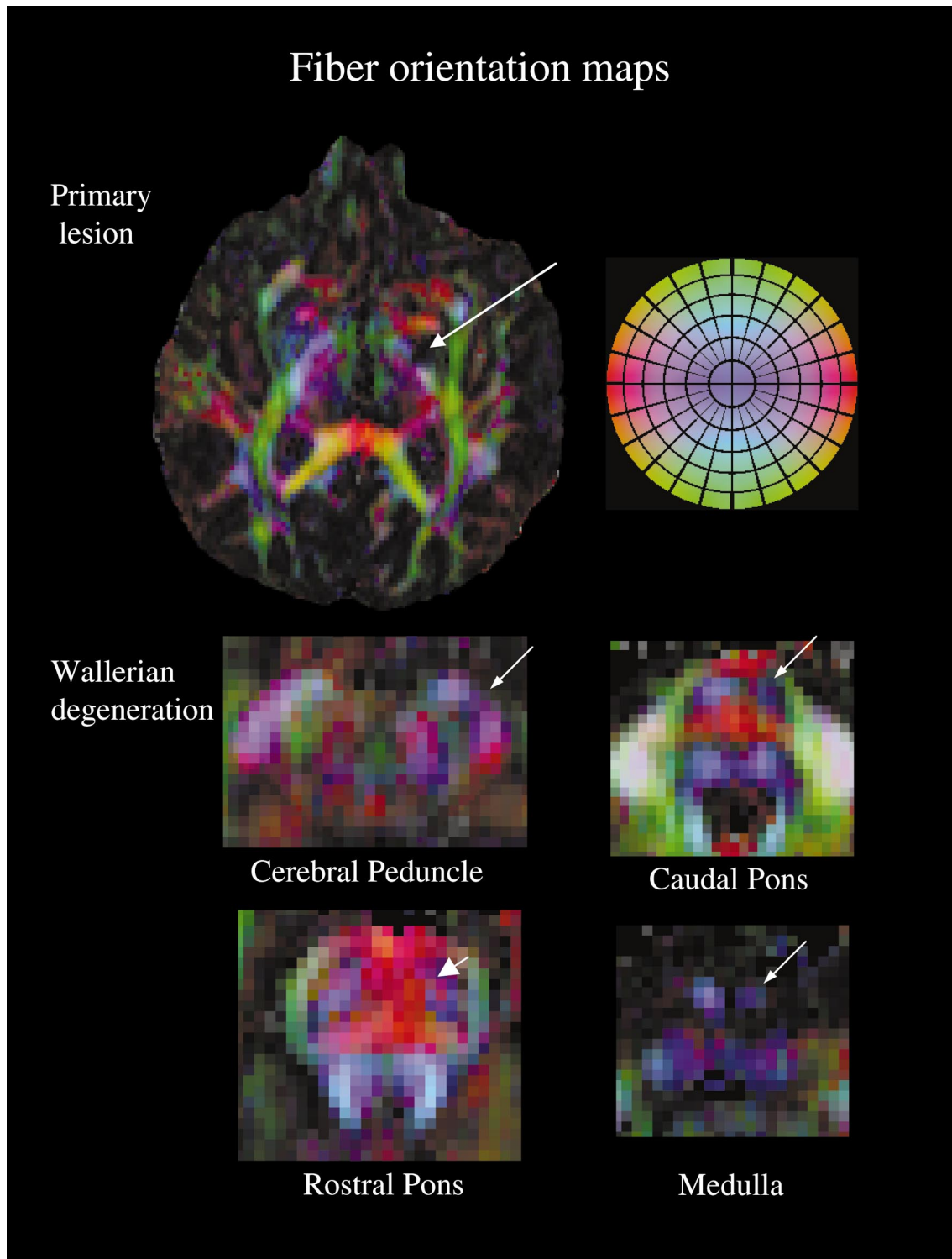


**FIG. 4.** Color coded fiber orientation maps obtained from of the same subjects shown in Figs. 2 and 3. The color-coding scheme is described in the Results. Arrows point to regions of Wallerian degeneration where diffusion anisotropy is reduced (lower brightness). In the rostral pons, however, Wallerian degeneration does not result in reduced anisotropy but in an apparent change in the orientation (color) of the fibers (arrowhead).

subjects either  $\epsilon_{1z}$ , or  $\epsilon_{1x}$ , or both  $\epsilon_{1z}$ , and  $\epsilon_{1x}$ , showed significant differences between healthy and affected sides in the rostral pons at the Mann–Whitney test.

Figure 5 shows computed trajectories of tracts in the motor pathways in both the healthy and lesioned sides of a representative subject. Trajectories are launched

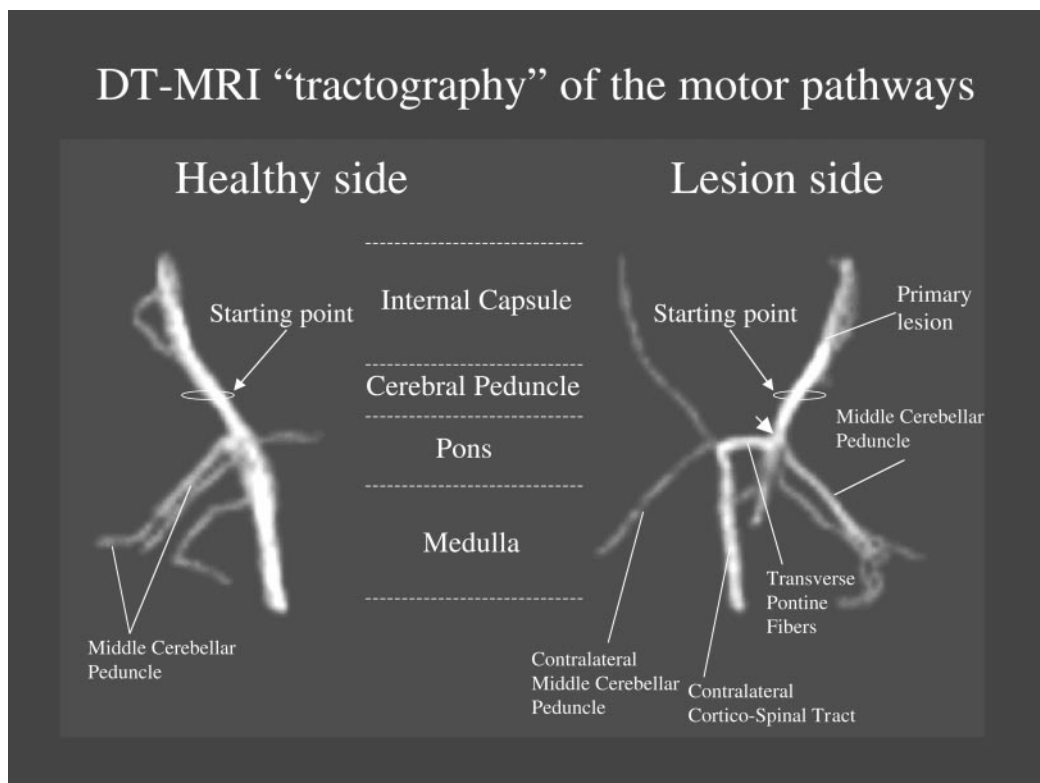


**FIG. 5.** Trajectories of the motor pathways computed from DT-MRI data by using an algorithm that follows a tract by tracing a path along which the local diffusivity is a maximum. Trajectories are launched in both the healthy and lesioned sides in superior and inferior directions starting from ROIs located at the level of the cerebral peduncle. While in the healthy side the algorithm highlights plausible trajectories of the motor pathways, in the side where Wallerian degeneration occurred reconstructed trajectories cross over to the contralateral side at the level of the pons, and continue along the contralateral middle cerebellar peduncle and contralateral motor pathways.

in both superior and inferior directions starting from ROIs at the level of the internal capsule. In the healthy side, the majority of fibers track the motor pathway. In the lesioned side, however, the majority of fiber track the primary motor pathway only until the level of the pons, and then abruptly turn to follow the transverse pontine fibers. Then, they turn again to follow the contralateral cortical spinal tract.

## DISCUSSION

Several previous works have reported that diffusion tensor MRI can detect degeneration of white matter fibers (Pierpaoli *et al.*, 1996a, 1998; Jones *et al.*, 1999; Wieshmann *et al.*, 1999a, 1999b). To our knowledge, however, a quantitative comparison between the sensitivity of DT-MRI- and T2-weighted imaging has not been performed. Our results show that both DT-MRI- and T2-weighted imaging detected statistically significant differences between the affected and healthy sides when the entire data set is considered. From a clinical standpoint, a more important question, however, is whether a technique can detect such pathology in a single subject. When we performed the statistical analysis using pooled data from all the ROIs for each

subject, T2-weighted imaging proved to be much less sensitive than DT-MRI. In fact, significant differences between healthy and affected sides in T2-weighted signal intensity were found in less than 50% of the subjects, while significant differences in diffusion anisotropy were found in all subjects. Interestingly, DT-MRI proved to be very sensitive even when a specific anatomical ROI was investigated. Diffusion anisotropy was significantly different in all comparisons involving a single ROI in a single subject except in the rostral pons ROIs. However, in the rostral pons other diffusion parameters, such as the local orientation of the fiber tracts (i.e., the eigenvector associated with the largest principal diffusivity) showed significant differences between the healthy and affected sides in all subjects.

The fact that water diffusion properties are altered throughout each individual pathological ROI indicates that DT-MRI has the potential of mapping the entire degenerated pathway in a single subject. Considering how postmortem studies of degenerated white matter have been fundamental for our understanding of the functional anatomy of many white matter pathways, one can appreciate the potential importance of now being able to perform such studies noninvasively *in vivo*.

The interpretation of the diffusion data, however, is not simple. Consistent with previously reported preliminary findings (Pierpaoli *et al.*, 1998), our study indicates that diffusion changes following Wallerian degeneration depend on the preexisting local architecture of the affected white matter pathways. In fact, diffusion changes observed in the rostral pons, a region where the descending motor pathways intersect the transverse pontine fibers, are quite different from the changes observed in the cerebral peduncle, a region where the descending motor pathways run as isolated and well-defined bundles of parallel fibers.

If we consider only white matter tracts having architectural features similar to that of the motor pathways in the cerebral peduncle, we identify the following DT-MRI "signatures" of Wallerian degeneration: severely reduced anisotropy, slightly increased Trace(**D**), reduced diffusivity parallel to the fibers (largest eigenvalue), increased diffusivity perpendicular to the fibers (smallest and intermediate eigenvalues). The finding of severely reduced anisotropy is consistent with results of previous DT-MRI studies (Pierpaoli *et al.*, 1996a, 1998; Jones *et al.*, 1999; Wiesmann *et al.*, 1999a, 1999b).

Our study shows that DT-MRI changes observed in regions of Wallerian (secondary) degeneration are different in many aspects from those observed in regions directly affected by the stroke (Primary lesion). While in both the primary lesion and the areas of Wallerian degeneration diffusion anisotropy is reduced, Trace(**D**) is greatly increased in the primary lesion and only slightly increased in Wallerian degeneration. Moreover, the diffusivity parallel to the fibers (largest eigenvalue) is increased in the primary lesion but reduced in Wallerian degeneration.

These differences in the changes in diffusion properties in primary and secondary white matter degeneration reflect structural differences in the two conditions. In regions primarily affected by the stroke, the resolution of the liquefactive necrosis leads to the formation of cystic spaces filled by CSF. The increased content of unhindered, isotropically diffusing water in these cavities is consistent with a marked increase in Trace(**D**) and the global increase of the diffusivity in all directions observed in the primary lesion. On the contrary, in Wallerian degeneration there is neither significant water accumulation in the interstitial spaces nor formation of cysts, even of microscopic dimensions. This is consistent with the limited increase in Trace(**D**) observed in this condition.

Axonal loss has been generally considered to be the main determinant of the decrease in diffusion anisotropy in Wallerian degeneration. We argue that fiber loss per se, without gliosis or an accompanying increase in extracellular matrix, would be insufficient to produce a decrease in diffusion anisotropy. In fact if the space occupied by degenerated fibers is simply replaced

by neighboring fibers that are still intact we expect a reduced volume of anisotropic tracts but not a reduction of the measured diffusion anisotropy. The reduction in diffusion anisotropy, accompanied by decreased diffusivity parallel to the fibers, increased diffusivity perpendicular to them, and a relatively small change in Trace(**D**), taken together, suggest that there is an increase in isotropic tissue structures in the regions where Wallerian degeneration has occurred. This is consistent with the presence of gliosis and the possible increase in extracellular matrix found histologically in Wallerian degeneration.

The limited increase in Trace(**D**) (overall only 10% in our group of patients) and the reduction in the diffusivity parallel to the fibers that we observed in Wallerian degeneration are key elements with which to differentiate pure secondary white matter degeneration from conditions in which fiber loss results from direct injury to the fiber tract or from conditions characterized by an inflammatory response in which interstitial water accumulation occurs, such as in multiple sclerosis (MS). The increase in Trace(**D**) that has been reported in chronic MS lesions (Horsfield *et al.*, 1998) and chronic stroke, including ischemic leukoaraiosis, a condition where primary and secondary fiber degeneration may coexist in the same region (Jones *et al.*, 1999), is generally much larger than that found in our study.

One of the main findings of this work is that diffusion changes following secondary white matter degeneration depend strongly on the preexisting architecture of white matter. The differences between the diffusion changes produced by Wallerian degeneration in regions with well-defined, isolated fiber bundles and in regions where fibers of the degenerated tract intersect other pathways are summarized in Table 2. In the latter regions a change in the apparent orientation of fibers, which is assumed to coincide with the orientation of the eigenvector associated to the largest eigenvalue ( $\epsilon_1$ ), not a change in diffusion anisotropy is the most relevant finding in Wallerian degeneration. These results can be explained by understanding how the degree of intravoxel orientational coherence of the fibers affects the measured diffusion tensor (Pierpaoli and Basser, 1996; Pierpaoli *et al.*, 1996b). In fact, the diffusion tensor that we measure with MRI, at the macroscopic scale of a voxel, reflects the contributions of all the microscopic tissue structures present within the voxel. If all axons within the voxel have the same orientation, then the direction of highest diffusivity measured with MRI will coincide with the orientation of the fiber tract.

However, if the axons are not coherently oriented within the voxel, as happens in regions of crossing pathways, the measured macroscopic tensor field will be a volume average of all microscopic domains. In such cases, diffusion anisotropy will be generally low and the direction of highest diffusivity will be a

TABLE 2

Summary of the Diffusion Changes Observed in the Chronic Stroke Lesion (Primary Lesion) and in Regions of Secondary (Wallerian) White Matter Degeneration

	Primary lesion	Wallerian degeneration in regions of isolated fiber bundles	Wallerian degeneration in regions of intersecting pathways
$D_{av} = \text{Trace}(\mathbf{D})/3$	Large increase	Small increase	Small increase
Diffusion anisotropy	Large decrease	Large decrease	Small decrease. No changes or slight increase possible
Diffusivity parallel to the fibers ( $\lambda_1$ )	Increase	Decrease	Small change
Diffusivity perpendicular to the fibers ( $\lambda_2$ and $\lambda_3$ )	Increase	Increase	Small change
Apparent fiber orientation ( $\epsilon_1$ )	Inconsistent changes due to loss of anisotropy	Inconsistent changes due to loss of anisotropy	Consistent changes dictated by the orientation of remaining pathways unaffected by Wallerian degeneration

*Note.* Diffusion changes following Wallerian degeneration are different depending on the preexisting architecture of white matter.

weighted average of the orientations of the different pathways. It has been previously shown in human subjects and nonhuman primates that the degree of orientational coherence of the fibers is an important determinant of diffusion anisotropy in normal brain (Pierpaoli and Basser, 1996; Pierpaoli *et al.*, 1996b). In normal brain, regions where fibers cross have much lower diffusional anisotropy than regions with coherently oriented fiber bundles. The rostral pons is one such region. The transverse pontine fibers, crossing the descending motor pathways with a left-right orientation, reduce the apparent anisotropy of the descending motor pathways at this level. Following Wallerian degeneration of the descending motor pathways, the transverse pontine fibers become the dominant pathway in the ROI and, paradoxically, the measured diffusion anisotropy can increase because fibers are now more coherently oriented within the voxel than they are in the normal case. Moreover, the direction of highest diffusivity or apparent direction of the fibers becomes more left-right oriented, like the transverse pontine fibers. Consistent with this interpretation, we observed a change in fiber orientation from superior-inferior to left-right in all our subjects. Diffusion anisotropy, however, increased only in one subject and decreased in the remaining cases, although much less than in the cerebral peduncle. Thus, the resulting changes in anisotropy following fiber degeneration in regions of fiber crossing is determined by two competing factors: increased orientational coherence of the remaining fibers tends to increase anisotropy, while gliosis and/or accumulation of extracellular matrix tend to reduce it. In different subjects these two factors may have a different preponderance leading to a small increase, no change or a small decrease in the measured diffusion anisotropy in these regions.

The implications of our findings go beyond the specific case of Wallerian degeneration. There is a widespread misconception that loss of white matter fibers is

always accompanied by a reduction in diffusion anisotropy. For example, the finding of low diffusion anisotropy in the frontal white matter of schizophrenic subjects has been interpreted as indicative of diminished fronto-striatal connectivity (Buchsbaum *et al.*, 1998). Our data show that this assumption may be incorrect in regions where white matter fibers are not arranged in well ordered bundles of parallel fibers.

In general, while structural and architectural features of the tissue do affect the diffusion behavior of water molecules, inferring histological characteristics from a given diffusion pattern is more problematic. This requires *a priori* knowledge of the structure and architecture of the tissue under investigation or at least a good hypothesis of about them.

We have shown, for example, that a state-of-the-art fiber tractography algorithm applied to the descending motor pathways produces anatomically incorrect fiber trajectories on the side where Wallerian degeneration occurred. Here, most of the reconstructed trajectories cross over to the contralateral side at the level of the pons, and continue in the contralateral middle cerebellar peduncle and contralateral motor pathways. In this case, we are able to discern that these computed pathways are artifactual. However, for many other pathways about which our anatomical knowledge is more limited, one may lack information required to interpret the diffusion findings correctly.

We must remember that DT-MRI fiber tractography and conventional histological tract-tracing techniques are based on very different physical principles. Conventional tract tracing techniques selectively label a specific pathway, while DT-MRI tractography follows the direction along which the voxel-averaged diffusivity is a maximum. If other structures are present in the voxel in addition to the pathway under investigation, the measured direction of highest diffusivity can deviate significantly from the true direction of the selected pathway. In other words, when conventional tract trac-

ing techniques show a given pathway connecting points A and B in the brain, we may be reasonably sure that this is a true anatomical connection. The same does not apply for DT-MRI tractography. A streamline of highest diffusivity may connect regions that have no anatomical connection between them. Anatomical connectivity may be suggested by a DT-MRI study but must be confirmed by using different means.

DT-MRI tractography algorithms are expected to perform more reliably with images acquired at higher spatial resolution. However, given that in many white matter regions fibers cross at a microscopic length scale, simply increasing spatial resolution will not improve the fidelity of the computed fiber tract trajectories in these regions. Improved DT-MRI tractography methods will have to be developed to address this important issue.

### Summary and Conclusions

We show that DT-MRI is more sensitive than T2-weighted imaging in detecting secondary white matter degeneration. Changes in diffusion parameters are found along the entire trajectory of the degenerated pathways and in all subjects suggesting that this technique could potentially be used for mapping fiber degeneration *in vivo*. We identify specific changes in diffusion parameters that appear characteristic of Wallerian degeneration in its chronic stage. These DT-MRI "signatures" of secondary white matter degeneration permit us to differentiate this condition from primary fiber loss following direct ischemic insult and from lesions of other diseases such as multiple sclerosis. In order to detect and characterize Wallerian degeneration, however, other DT-MRI parameters in addition to diffusion anisotropy need to be measured, including Trace(**D**), the principal diffusivities, and the principal directions of diffusion.

Previous studies have shown that diffusion anisotropy is severely reduced in Wallerian degeneration. We confirm this finding in regions where white matter fibers are arranged in parallel bundles. However, in regions where the degenerated pathway intersects other tracts, the decrease in diffusion anisotropy is smaller and more inconsistently observed in different subjects. In such regions a change in the apparent spatial orientation of the fibers is the most noticeable consequence of Wallerian degeneration.

The assessment of fiber degeneration with DT-MRI appears to be a promising tool for studying human neuroanatomy noninvasively *in vivo*. However, care is needed to interpret the diffusion imaging results, particularly to ensure that inferences about changes in tissue structure and architecture are correct.

### REFERENCES

- Aldroubi, A., and Basser, P. J. 1999. Reconstruction of vector and tensor fields from sampled discrete data. In *Contemporary Mathematics* (L. W. Baggett and D. R. Larson, Eds.), Vol. 247, pp 1–15. AMS, Providence, RI.
- Anderson, A. W., and Gore, J. C. 1994. Analysis and correction of motion artifacts in diffusion weighted imaging. *Magn. Reson. Med.* **32**(3): 379–387.
- Barnett, A. 1997. Improved reconstruction algorithm for navigator corrected diffusion weighted interleaved echo-planar images. *ISMRM Proc.* 1727.
- Basser, P. J. 1995. Inferring microstructural features and the physiological state of tissues from diffusion-weighted images. *NMR Biomed.* **8**(7–8): 333–344.
- Basser, P. J. 1998. Fiber-Tractography via Diffusion Tensor MRI (DT-MRI). *ISMRM Proc.* 1226.
- Basser, P. J., Mattiello, J., and LeBihan, D. 1994. MR diffusion tensor spectroscopy and imaging. *Biophys. J.* **66**(1): 259–267.
- Basser, P. J., Pajevic, S., Pierpaoli, C., Aldroubi, A., and Duda, J. 2000. *In vivo* fiber-tractography in human brain using diffusion tensor MRI (DT-MRI) data. *Magn. Reson. Med.* **44**(4): 625–632.
- Basser, P. J., and Pierpaoli, C. 1996. Microstructural and physiological features of tissues elucidated by quantitative-diffusion-tensor MRI. *J. Magn. Reson. B*(3): 209–219.
- Beaulieu, C., Does, M. D., Snyder, R. E., and Allen, P. S. 1996. Changes in water diffusion due to wallerian degeneration in peripheral nerve. *Magn. Reson. Med.* **36**(4): 627–631.
- Buchsbaum, M. S., et al. 1998. MRI white matter diffusion anisotropy and PET metabolic rate in schizophrenia. *Neuroreport* **3**: 425–430.
- Castillo, M., and Mukherji, S. K. 1999. Early abnormalities related to postinfarction Wallerian degeneration: Evaluation with MR diffusion-weighted imaging. *J. Comput. Assist. Tomogr.* **23**(6): 1004–1007.
- Cobb, S. R., and Mehlinger, C. M. 1987. Wallerian degeneration in a patient with Schilder disease: MR imaging demonstration. *Radiology* **162**(2): 521–522.
- Horsfield, M. A., Larsson, H. B., Jones, D. K., and Gass, A. 1998. Diffusion magnetic resonance imaging in multiple sclerosis. *J. Neurol. Neurosurg. Psychiatry* **64**(Suppl 1): S80–S84.
- Jezzard, P., Barnett, A. S., and Pierpaoli, C. 1998. Characterization of and correction for eddy current artifacts in echo planar diffusion imaging. *Magn. Reson. Med.* **39**(5): 801–812.
- Jones, D. K., Lythgoe, D., Horsfield, M. A., Simmons, A., Williams, S. C., and Markus, H. S. 1999. Characterization of white matter damage in ischemic leukoaraiosis with diffusion tensor MRI. *Stroke* **30**(2): 393–397.
- Jones, E. G. 1999. Making brain connections: Neuroanatomy and the work of TPS Powell, 1923–1996. *Annu. Rev. Neurosci.* **22**: 49–103.
- Kuhn, M. J., Johnson, K. A., and Davis, K. R. 1988. Wallerian degeneration: Evaluation with MR imaging. *Radiology* **168**(1): 199–202.
- Kuhn, M. J., Mikulis, D. J., Ayoub, D. M., Kosofsky, B. E., Davis, K. R., and Taveras, J. M. 1989. Wallerian degeneration after cerebral infarction: evaluation with sequential MR imaging. *Radiology* **172**(1): 179–182.
- Le Bihan, D. 1991. Molecular diffusion nuclear magnetic resonance imaging. *Magn. Reson. Q.* **7**(1): 1–30.
- Makris, N., et al. 1997. Morphometry of *in vivo* human white matter association pathways with diffusion-weighted magnetic resonance imaging. *Ann. Neurol.* (6): 951–962.

- Mattiello, J., Basser, P. J., and Le Bihan, D. 1997. The b matrix in diffusion tensor echo-planar imaging. *Magn. Reson. Med.* **37**(2): 292–300.
- Ordidge, R. J., Helpert, J. A., Qing, Z. X., Knight, R. A., and Nagesh, V. 1994. Correction of motional artifacts in diffusion-weighted MR images using navigator echoes. *Magn. Reson. Imag.* **12**(3): 455–460.
- Pajevic, S., and Basser, P. J. 1999. Non-parametric statistical analysis of diffusion tensor MRI data using the bootstrap method. *ISMRM Proc.* 1790.
- Pajevic, S., and Pierpaoli, C. 1999. Color schemes to represent the orientation of anisotropic tissues from diffusion tensor data: Application to white matter fiber tract mapping in the human brain. *Magn. Reson. Med.* **42**(3): 526–540.
- Pierpaoli, C. 1997. Oh no! One more method for molor mapping of fiber tract direction using diffusion MR imaging data. *ISMRM Proc.* 1741.
- Pierpaoli, C., Barnett, A., Penix, L., De Graba, T., Basser, P. J., and Di Chiro, G. 1996a. Identification of fiber degeneration and organized gliosis in stroke patients by diffusion tensor MRI. *ISMRM Proc.* 563.
- Pierpaoli, C., Barnett, A., Virta, A., Penix, L., and Chen, R. 1998. Diffusion MRI of Wallerian degeneration. A new tool to investigate neural connectivity *in vivo*? *ISMRM Proc.* 1247.
- Pierpaoli, C., and Basser, P. J. 1996. Toward a quantitative assessment of diffusion anisotropy. *Magn. Reson. Med.* **36**(6): 893–906.
- Pierpaoli, C., Jezzard, P., Basser, P. J., Barnett, A., and Di Chiro, G. 1996b. Diffusion tensor MR imaging of the human brain. *Radiology* **201**(3): 637–648.
- Salonen, O., Autti, T., Raininko, R., Ylikoski, A., and Erkinjuntti, T. 1997. MRI of the brain in neurologically healthy middle-aged and elderly individuals. *Neuroradiology* **39**(8): 537–545.
- Sawlani, V., Gupta, R. K., Singh, M. K., and Kohli, A. 1997. MRI demonstration of Wallerian degeneration in various intracranial lesions and its clinical implications. *J. Neurol. Sci.* **146**(2): 103–108.
- Segawa, F., Kinoshita, J., Kishibayashi, K., Kamada, K., Sunohara, K., Shimizu, Y., and Hashimoto, Y. 1993. Diffusion images of Wallerian degeneration. *SMRM Proc.* 595.
- Stovring, J., and Fernando, L. T. 1983. Wallerian degeneration of the corticospinal tract region of the brain stem: Demonstration by computed tomography. *Radiology* **149**(3): 717–720.
- Tievsky, A. L., Wu, O., Gonzalez, R. G., Rosen, B. R., and Sorensen, A. G. 1998. ADC and diffusion anisotropy indices in wallerian degeneration. *Rivista Di Neuroradiologia* **11**: 130–134.
- Virta, A., Barnett, A. L., and Pierpaoli, C. 1999. Visualizing and characterizing white matter fiber structure and architecture in the human pyramidal tract using diffusion tensor MRI. *Magn. Reson. Imag.* **17**(8): 1121–1133.
- Wahlund, L. O., Almkvist, O., Basun, H., and Julin, P. 1996. MRI in successful aging, a 5-year follow-up study from the eighth to ninth decade of life. *Magn. Reson. Imag.* **14**(6): 601–608.
- Wieshmann, U. C., Clark, C. A., Symms, M. R., Franconi, F., Barker, G. J., and Shorvon, S. D. 1999a. Anisotropy of water diffusion in corona radiata and cerebral peduncle in patients with hemiparesis. *NeuroImage* **10**(2): 225–230.
- Wieshmann, U. C., Symms, M. R., Clark, C. A., Lemieux, L., Franconi, F., Parker, G. J. M., Barker, G. J., and Shorvon, S. D. 1999b. Wallerian degeneration in the optic radiation after temporal lobectomy demonstrated *in vivo* with diffusion tensor imaging. *Epilepsia* **40**(8): 1155–1158.